Available online at www.sciencedirect.com
ScienceDirect
Journal of Nuclear Materials 372 (2008) 177–181
journal of nuclear materials
www.elsevier.com/locate/jnucmat

SCC and corrosion evaluations of the F/M steels for a supercritical water reactor

Seong Sik Hwang [a,*], Byung Hak Lee [a], Jung Gu Kim [b], Jinsung Jang [a]

[a] Korea Atomic Energy Research Institute, 150 Deokjin-dong, Yuseong-gu, Daejeon, Republic of Korea
[b] Department of Advanced Materials Engineering, SungKyunKwan University 300 Chunchun-Dong, Jangan-Gu, Suwon 440-746, Republic of Korea

Received 20 November 2006; accepted 14 March 2007

Abstract

As one of the Generation IV nuclear reactors, a supercritical water cooled reactor (SCWR) is being considered as a candidate reactor due to its high thermal efficiency and simple reactor design without steam generators and steam separators. For the application of a structural material to a core's internals and a fuel cladding, the material should be evaluated in terms of its corrosion and stress corrosion cracking susceptibility. Stress corrosion cracking and general corrosion tests of ferritic–martensitic (F/M) steels, high Ni alloys and an oxide dispersion strengthened (ODS) alloy were performed. Stress corrosion cracking (SCC) was not observed on the fractured surface of the T 91 steel in the supercritical water at 500, 550 and 600 °C. As the test temperature increased, the ultimate tensile strength (UTS) and yield strength (YS) of T 91 decreased, and a high dissolved oxygen level induced corrosion and low ductility. The F/M steels showed a high corrosion rate whereas the Ni base alloys showed a little corrosion at 500 and 550 °C. Corrosion rate of the F/M steels at 600 °C test was up to three times larger than that at 500 °C. A thin layer composed of Mo and Ni seems to retard the Cr diffusion into the out layer of the corrosion product of T 92 and T 122.

PACS: 82.45.Bb; 28.41.Te; 81.65.Mq; 68.37.Hk

1. Introduction

As one of the Generation IV nuclear reactors, a supercritical water cooled reactor (SCWR) is being considered as a candidate reactor due to its high thermal efficiency and simple reactor design without steam generators and steam separators [1,2]. At above the supercritical condition of 374 °C, 22.1 MPa, the supercritical water does not change its phase through out the reactor core outlet. Therefore, the high temperature coolant is effectively used at over a 40% thermal efficiency [3–5].

An elimination of reactor components such as the steam generators and steam separators is another advantage of the SCWR when compared to normal LWRs [6]. Various different properties from those at a normal liquid state at room temperature such as a dielectric constant, an ionic product and a heat capacity are of major concern for the application of critical water to industrial utilities [7,8]. A critical step for this good feature to be attainable is to choose a proper structural material. For the application of a structural material to a core's internals and a fuel cladding, the material should be evaluated in terms of its tensile strength at a high temperature, creep strength, corrosion and stress corrosion cracking susceptibility, radiation resistance, weldability, etc. [9]. Among the qualification items, corrosion and stress corrosion cracking (SCC) tests of F/M steels have been performed in a supercritical water environment in the present work.

The present work aims at evaluating the corrosion behavior and the SCC behavior of F/M steels as the candidate material for the SCWR.

* Corresponding author. Tel.: +82 42 868 2310; fax: +82 42 868 8696.
E-mail address: sshwang@kaeri.re.kr (S.S. Hwang).

0022-3115/$ - see front matter © 2007 Elsevier B.V. All rights reserved.
doi:10.1016/j.jnucmat.2007.03.168

2. Experimental

The SCC behaviors of two F/M steels (T 91a, T 92) were evaluated in a supercritical water environment. Deionized water (~0.05 μS/cm) of below 10 ppb of dissolved oxygen and about pH 6.5 was used as a test solution. SCC tests using a slow strain rate tester (SSRT) and U-bend specimens were carried out at 500, 550 and 600 °C. The surface of the U-bend specimens was polished with up to a 0.3 μm alumina powder before U shape bending. The SSRT specimens were ground with #600 SiC emery paper on their gauge section followed by a cleaning with acetone. The SCC tests using the U-bend and the SSRT specimens were carried out simultaneously in the same autoclave. After the tests, a gauge section of the SSRT specimen was observed with a scanning electron microscope (SEM) to confirm a SCC occurrence. The cross sections of the U-bend specimens were also analyzed with a SEM.

The general corrosion resistance of three groups of materials such as F/M steels (T 91a, T 91b, T 92, T 122), high Ni alloys (alloy 625, 690, Incoloy 800H) and an ODS alloy (MA 956, a commercial 20% Cr ODS alloy) was evaluated in the same supercritical water environment as the SCC test. Table 1 shows the chemical composition of the test materials. Test coupons shown in Table 2 were immersed in a supercritical water environment, and test conditions of the corrosion rate measurement are summarized in Table 3. A cross section of the corrosion coupons was analyzed with a SEM and energy dispersive X-ray spectroscopy (EDS).

The corrosion and SCC test loop of the supercritical water environment designed for operation at 650 °C, 30 MPa is schematically shown in Fig. 1. It consists of a pressure vessel of a 3.3 liter volume capacity made of Hastelloy C-276, a make up water control loop, a SSRT control unit and a data acquisition module.

Table 2
Test materials and dimensions of the coupons for the corrosion rate measurement

Alloy class	Alloy	Shape
Ferritic–martensitic steels	T 91a, T 91b, T 92, T 122	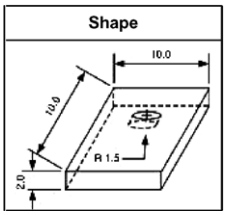
High Ni alloys (superalloys)	Inconel 625, Inconel 690, Incoloy 800H	
ODS alloy	MA 956	

Table 3
Test conditions of the corrosion rate measurement

Environments	Subcritical and supercritical water
Temperature (°C)	370, 400, 500, 600
Pressure (kgf/cm)	25
O_2 (ppb)	<10 (deaerated)
Test times (h)	200
Inlet conductivity (μS/cm)	<0.1
pH	Neutrality (6.4–6.9)
Flow rate (cc/min)	<10

Table 1
Chemical compositions (wt%) of the alloys for the general corrosion tests

Alloy	Fe	C	Si	Mn	P	S	Cr	Ni	Mo	–
	–	V	Nb	W	Ti	Al	N	O	Cu	Others
T 9la	Bal	0.084	0.438	0.363	0.019	0.0008	8.876	0.102	0.928	–
	–	0.197	0.081			0.016	0.0351		0.081	
T 91b	Bal	0.1	0.28	0.45	0.01	0.003	8.37	0.21	0.9	–
	–	0.22	0.08			0.02	0.048		0.17	
T 92a	Bal	0.07		0.46			9		0.5	–
	–	0.2	0.05	1.8			0.06			
T 92b	Bal	0.11	0.18	0.43	0.016	0.002	8.91	0.12	0.47	–
	–	0.19	0.06	1.67		0.004	0.043			0.003B
T 122	Bal	0.1	0.27	0.58	0.017	0.002	12.12	0.35	0.35	–
	–	0.19	0.06	1.84		0.014	0.07		0.83	0.003B
MA 956	Bal	0.02	0.04	0.1	0.01	0.008	19.4	0.05		–
	–				0.32	4.8	0.022	0.23	0.02	0.52
Inconel 625	4.52	0.02	0.17	0.1	0.01	<0.001	21.8	60.04	9.02	–
	–		3.62		0.27	0.2			0.08	0.20 Co
Inconel 690	10.7	0.002	0.39	0.28	0.01	0.002	29.8	58.3	0.01	–
	–				0.34	0.02	0.032		0.010	0.001 Ta
Incoloy 800H	47.6	0.07	0.4	0.74	0.01	<0.001	19.4	31.1		–
	–				0.32	0.23			0.1	0.05 Co

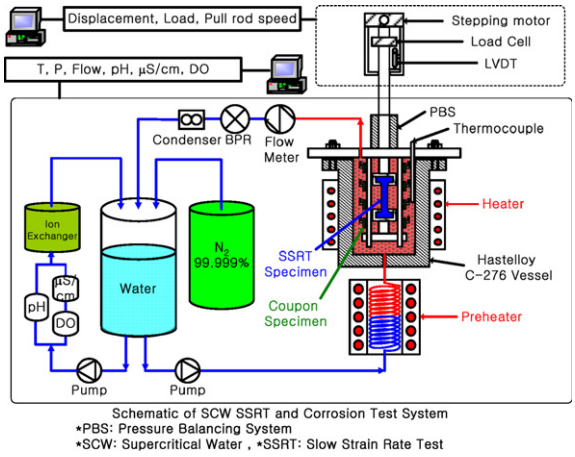

Fig. 1. Corrosion and SCC test loop of the supercritical water environment.

3. Results and discussion

3.1. Temperature dependency of a SCC

T 91 steels did not show SCC in the SSRT test at 550, and 600 °C, instead they exhibited an oxide film rupture at the necking area as shown in Fig. 2. Fournier et al. also performed a SCC test on alloy 690, and a ductile feature with a cracking of the oxide at the gauge section found in their experiment was similar to that found in this study [10]. The specimens also failed in a ductile fracture mode at 500 °C. As the test temperature increased, the ultimate tensile strengths (UTS) and yield strengths (YS) of the T 91 alloy decreased as shown in Fig. 3.

Strain rates at 500 °C and 550 °C were $1.5 * 10^{-7}\,s^{-1}$ and $3.0 * 10^{-7}\,s^{-1}$, respectively. It has been reported that the maximum stress increased as the strain rate increased for alloy 600 in a high temperature water [11]. In the present test, alloy T 91 showed lower UTS at a faster straining rate of $3.0 * 10^{-7}\,s^{-1}$ than at a slower straining rate of $1.5 * 10^{-7}\,s^{-1}$. The lower UTS at the faster strain rate of alloy T 91 seems to be due to the high test temperature of 550 °C; the increase of the strain rate did not give rise to an increase of the UTS. Compared with the UTS at 550 °C, the low UTS at 600 °C explains the dominant effect of the test temperature on the tensile properties. The elongations were similar (about 20%) regardless of the test temperatures.

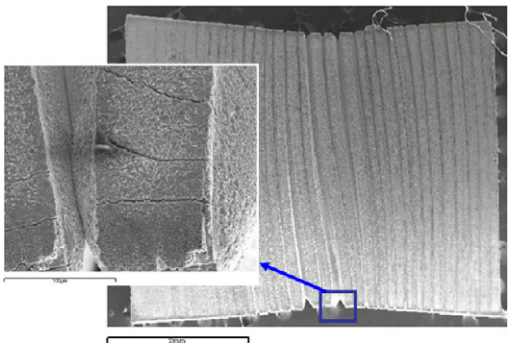

Fig. 2. Feature of a necking of T 91a tested at 500 °C by using an SSRT.

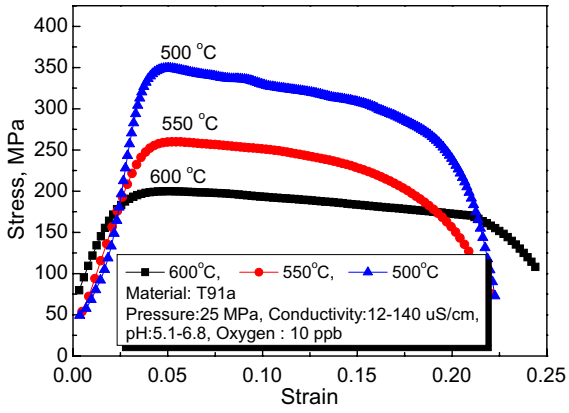

Fig. 3. Effect of the test temperature on the stress–strain curves of the alloy T 91a in a supercritical water.

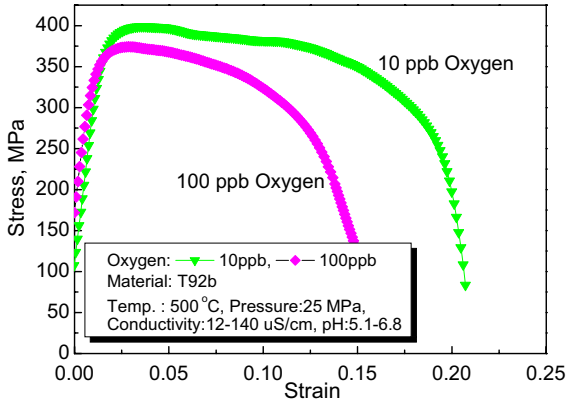

Fig. 4. Effect of the dissolved oxygen content on the stress–strain curves of alloy 91a in a SCW.

Alloy 91a tested in a 100 ppb dissolved oxygen (D.O.) content showed a little lower UTS than that in the 10 ppb D.O. as shown in Fig. 4. An elongation, however, decreased a lot as the D.O. level was increased. This implies that the high D.O. content caused a high oxidation reaction on the surface of the test specimen, resulting in a low ductility of the material.

3.2. Material dependency of a SCC

Fig. 5 shows the material dependency of the tensile strength of the F/M steels in the SCW. Alloy T 92b showed a higher UTS than that of T 91a at 500 °C at the same strain rate of $1.5 * 10^{-7}\,s^{-1}$; 399 MPa for T 92b, 349 MPa for T 91a. It is believed that the addition of W and N to alloy 92B increased its UTS. It seems to be necessary to undertake systematic tests to understand the effects of minor elements.

U-bend specimens of T 91 did not show any cracking at the apex of the U-bend regardless of the test temperature at 500 °C and 550 °C.

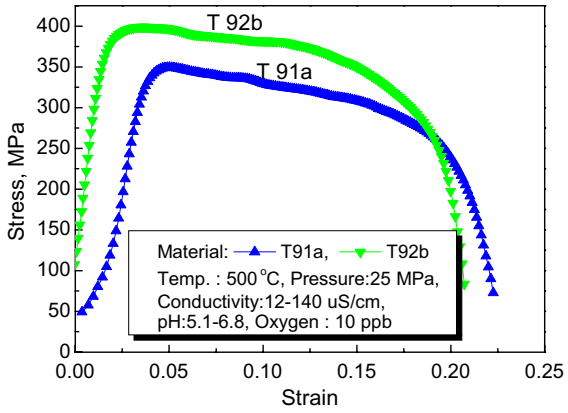

Fig. 5. Material dependency of the stress–strain curves of the F/M steels in a SCW.

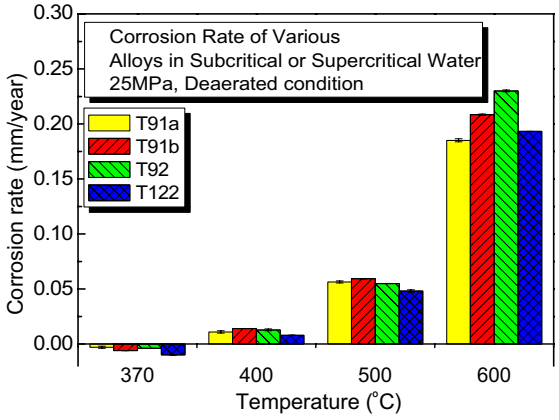

Fig. 7. Effect of the test temperature on the corrosion rate of the candidate alloys for a SCWR.

3.3. Material dependency of general corrosion

The F/M steels showed a corrosion rate as a form of a weight gain, and the steels showed a higher corrosion rate than the Ni alloys at the supercritical conditions as shown in Fig. 6. The big difference in the corrosion rates between the two groups (F/M steels and Ni alloys) seems to be from a dissolution behavior of the main alloying elements which are Fe for the F/M steels, and Ni for the Ni alloys. The F/M steels showed a smaller corrosion rate at 400 °C. At the subcritical condition of 370 °C, the F/M steels showed a weight loss. On the other hand, alloy MA 956, Incoloy 800H and the Ni base alloys showed a little weight change before and after the immersion test regardless of the test temperatures; subcritical or supercritical water.

A main factor for the general corrosion rate was the test temperature as shown in Fig. 7. The corrosion rates of the F/M steels at 600 °C were about three times larger than those at 500 °C. The high Cr content of the alloy 122 seems to show a lower corrosion rate than that of the alloy T 91, but it was less effective than the test temperature.

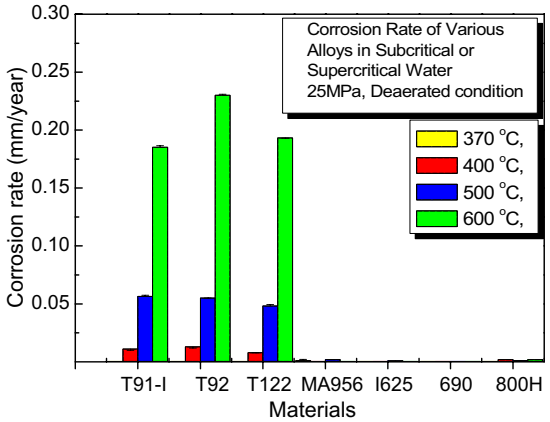

Fig. 6. Material dependency of the corrosion rate of various alloys in deaerated subcritical or supercritical water.

There was a small difference in the corrosion layer thickness or the corrosion rates of the T 92 and T 122 samples, which had different Cr contents (9% and 12%, respectively).

3.4. Corrosion product analysis

Oxide of the alloy T 91 was composed mainly of three layers as shown in Fig. 8. There was a thin layer (L3 on the micrograph) between layers 2 and 4, which was enriched in Mo and Ni. A distinct element variation was measured in layers 2 and 3; depletion of Fe with an enrichment of Cr was shown in layer 2, depletion of Cr with an enrichment of Mo was detected in layer 4. Layer 3 enriched in Mo seems to retard an outward Cr diffusion. A source of the Mo in layer 3 seems to be the alloying element of T 91 and the test vessel material of Hastelloy C 276. An ion exchanger to purify the test solution was not installed for this corrosion test, so the Mo from the test vessel is considered to be dissolved and deposited onto the corrosion

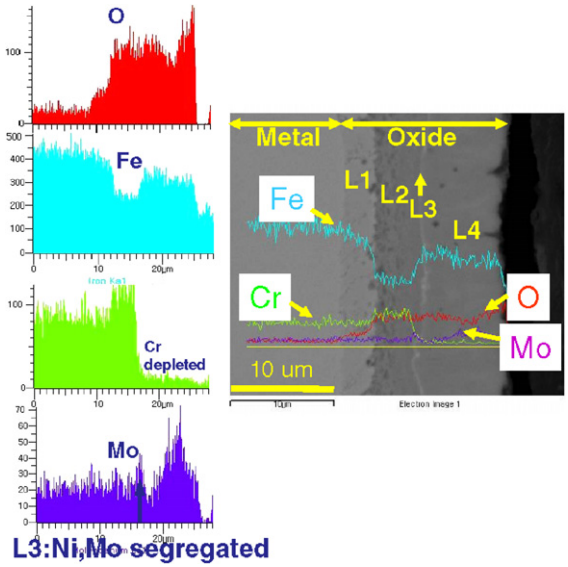

Fig. 8. Micrographs of the oxide on the T 91 sample tested in a SCW at 550 °C/25 MPa (D.O.<10 ppb).

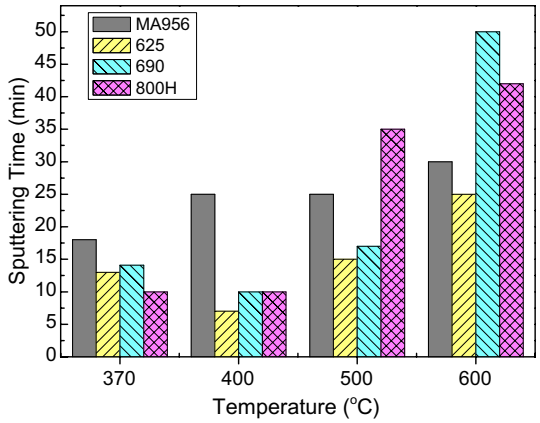

Fig. 9. Comparison of oxide thickness of the alloys formed in sub critical and super critical water (25 MPa, D.O.<10 ppb).

Table 4
Summary of the corrosion product analysis on each alloy

Alloys	Oxide thickness	Oxide layer
F/M steels (T 91, T 92, T 122)	~10 μm Thick	Mo Segregated, a boundary between Fe and Cr oxide Outside of Mo segregated layer: Cr depleted
Ni base alloys. Incoloy 800H	Very thin (less than 1 μm)	Not analyzed by EDS

product. Alloy T 92 and alloy T 122 showed a similar elemental profile to T 91. Was et al. reported a similar behavior of a layered structure of an oxide in type 304L Stainless steel for a 550 °C test in SCW [5].

On the surfaces of the alloy MA 956, alloy 625, alloy 690, and Incoloy 800H, thin oxides were formed. A small amount of oxide was formed on the alloy 625 surface, so the main alloying elements did not change at the surface. Another research group has also reported a similar result for the corrosion of alloy 625 [5,6]. Fig. 9 shows a comparison of oxide thickness of MA 956, Ni alloys and Incoloy 800H in the sub critical and super critical water. Summary of the corrosion product analysis is shown in Table 4.

4. Conclusions

- No SCC was observed on the fractured surface of the T 91 steel in the supercritical water at 500, 550 and 600 °C.
- As the test temperature increased, the UTS and YS of T 91 decreased.
- High dissolved oxygen level induced corrosion and a low ductility of the F/M steel, T 92b.
- Due to the addition of W, Alloy 92b showed higher UTS than that of alloy 91a.
- The F/M steels showed a high corrosion rate whereas the Ni base alloys showed a significantly smaller corrosion rate at 500 and 550 °C.
- Corrosion rate in supercritical water at 600 °C was up to three times larger than that of at 500 °C for the F/M steels.
- A thin layer composed of Mo and Ni seems to retard the Cr diffusion into the out layer of the corrosion product of T 92 and T 122.

Acknowledgements

The research was sponsored by the Ministry of Science and Technology, Korea under the National Mid- and Long-term Atomic Energy R&D Program. The authors acknowledge V&M Tubes, France for providing of sample materials.

References

[1] K. Kataoka et al., in: Proceedings of ICAPP 03, Cordoba, Spain, 4–7 May, 2003.
[2] D. Squarer, T. Schulenberg, D. Struwe, Y. Oka, D. Bittermann, N. Aksan, C. Maraczy, R. Kyrki-Rajamäki, A. Souyri, P. Dumaz, Nucl. Eng. Des. 221 (2003) 167.
[3] Y. Oka, S. Koshizuka, SCR-2000, 6–8 November 2000, Tokyo, The University of Tokyo, 2000, p. 1.
[4] J. McKinley, S. Teysseyre, G.S. Was, D.B. Mitton, H. Kim, J.-K. Kim, R.M. Latanision, GENES4/ANP2003, 15–19 September, 2003, Kyoto, Japan, Paper No. 1027.
[5] G.S. Was, S. Teysseyre, J. McKinley, in: NACE's International Conference, Corrosion 2004, New Orleans, Paper No. 04492, 2004.
[6] S. Teysseyre, J. McKinley, G.S. Was, D.B. Mitton, H. Kim, J.-K. Kim, R.M. Latanision, in: Proceedings of 11th International Symposium on Environmental Degradation of Materials in Nuclear Power Systems – Water Reactors, Stevenson, WA, 10–14 August, 2003, Paper No. 71221.
[7] P. Kritzer, SCR-2000, 6–8 November, 2000, Tokyo, The University of Tokyo, 2000, p. 1.
[8] Y. Watanabe, H. Abe, Y. Daigo, GENES4/ANP2003, 15–19 September, 2003, Kyoto, Japan, Paper 1183.
[9] J. Jang, W.S. Ryu, J.H. Hong, in: Proceedings of 6th Conference on Mechanical Behavior of Materials, Jeju, Korea, 8 November, 2002, p. 425.
[10] L. Fournier, D. Delafosse, C. Bosch, Th. Magnin, in: NACE's International Conference, Corrosion 2001, Houston, TX, Paper 01361, 2001, p. 1.
[11] R.N. Parkins, in: G.M. Urgiansky, J.H. Payer (Eds.), Stress Corrosion Cracking – The Slow Strain Rate Technique, ASTM-STP-665, 1979, p. 5.